

Specific Adhesion and Piezocoefficient under Dry and Boundary Friction 233
 Yu.N. Vasiliev, D.A. Gorbunov, V.A. Fugol, V.I. Kostikov

On the Mechanism of Interaction of Transport Means Wheels with Rails 237
 Yu.M. Luzhnov, A.V. Chichinadze

Effect of a Rigid Mounting of a Polymer Friction Element on Its Compliance during Friction 245
 N.I. Zharovcoev

About Application of Mechatronic Systems in Tribotechnique 251
 A.V. Sokolov

MECHANISM OF FRICTION AND WEAR

Friction and Wear Mechanism of Some Asbestos-Free Friction Composites 256
 A.K. Pogosian, N.G. Meliksetian, N.A. Lembarian

Wear of Polytetrafluoroethylene Containing the Solid High-Dispersive Filler 261
 A.V. Vinogradov, Yu.V. Demidova, O.A. Adrianova, A.A. Okhlopko, A.I. Gerasimov

Friction and Wear in Groups of the Chain Drives from Polymer Composites 273
 O.I. Filipenko

The Influence of Structural Components Thin Structure upon the Destruction Mechanism of Composite Materials 279
 I.M. Spiridonova, E.V. Sukhovaja, V.A. Zaborovsky

On the Relationship of Abrasive Wear Resistance of Metals to the Parameters of the Hardening Curves 282
 V.A. Krocha, V.E. Planida

Contact Interaction and Wear Examination of the Wheel-Rail Couple 288
 V.P. Bessacolev, A.V. Sladkovsky

SURFACE PHYSICS

Influence of Reciprocating Sliding on the Running-in of Lubricated Concentrated Contacts 295
 D.J. Schipper, P.H. Vroegop, A.W.J. de Gee

Mathematical Model of Heat Exchange between Frictioning Drum and Brake Linings 296
 A.D. Petrov, A.V. Chichinadze

Methods of Determining Tribologic Properties of Materials Based on the In-Process and On-Line Measurements of the Electron Work Function of Rubbing Surfaces 302
 A.L. Zharin, E.I. Fishbein, N.A. Shipitsa

Rated Energy Limit of "Thin" Lubrication Disks 319
 V.S. Revoko, G.M. Plidlider

Friction Properties of Carbon-Carbon Composites 327
 V.V. Kulakov, A.M. Kenlgfest, I.V. Zchak, A.G. Sokker, I.V. Rastorgueva, M.V. Maljutin, A.V. Suvorov, S.H. Kim, E.N. Sisikova

Plasma Formation of Wear Resistance Ceramic and Titanium Coatings 332
 O.A. Yakubtsov, V.D. Parkhomenko, I.A. Molchanovskii

The Combined Methods of Frictional Parts and Units Surfaces Forming 338
 A.V. Borisenko, N.N. Popok, M.L. Kheifets

Ways of Increasing Efficiency of Processes Forming Surfaces of Friction 344
 M.L. Kheifets

CONTACT INTERACTION AND WEAR EXAMINATION
OF THE WHEEL - RAIL COUPLE

V.P. Essaoolov, A.V. Sladkovsky

Dnepropetrovsk

The Dnepropetrovsk Metallurgical Institute

The development of railway transport in the USSR determines the modernization of railway track and track vehicle interaction. This relates first of all to the idea of creation of high-speed movement transport means. The successful realization of this project means the regulation of wheel-rail interaction problem as well. This problem became acute in recent years.

One of the possible ways of solution one can distinguish in modernization of constructive design of wheel and rail working surfaces. Said modernization must promote contact stress decreasing, improvement of train dynamic stability and consecutive wear rate reduction of coupling items. The European UIC investigated local conditions and developed a number of Standarts for wheel and rail profiles. The rails in Europe are stated to be of curvilinear shape. The wheel profile with piece-and-linear shape is still used in the USSR.

For many years the Dnepropetrovsk Metallurgical Institute (DMetI) carries out researches directed to the ways of implementation of wheel-to-rail effective interaction and have managed to develop new designs for rails and wheels. Thus, a mathematical model for a single wheel pair run along a circular curve with regard to the actual wheel and rail profiles was elaborated. Above model helps to study the conditions of wheel pairs entering circular curves.

The way of single wheel pair entering the curve having the outer rail height h_r is shown in Fig. 1. The circular curvature radius for this pair equals to R , and the gauge wheel value is $2s_1$. The wheel and rail working surfaces must be described in the coordinate system xoy connected with the gauge centre and turned to the angle $\alpha = \arcsin(h_r/2s_1)$. The most complicated appears to be the case when said surfaces display actual traces of wear. Then they are inscribed in the form of function:

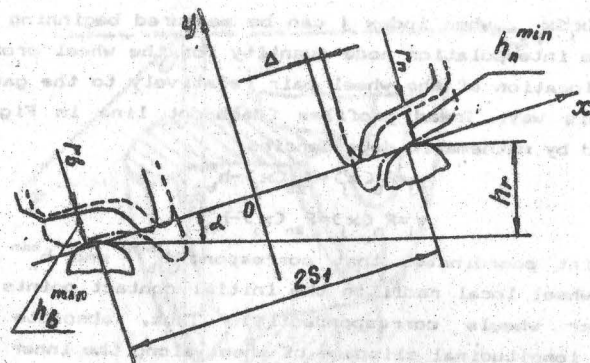


Fig. 1.

$$y_i = f_n(x_i), \quad y_i = f_b(x_i), \quad i=1, \dots, m. \quad (1)$$

Here, the first relation and index n refer to the outer rail, and the second relation and index b refer to the inner rail. The full line (Fig. 1.) presents the initial position of the wheel pair within the chosen coordinate system. For this

$$y_j = F_{1n}(x_j), \quad y_j = F_{1b}(x_j), \quad j=1, \dots, k. \quad (2)$$

where both the first and the second relation, as well as indexes n and b , refer to the outer and inner wheels, correspondently. Relation (1) and (2) must take into account the actual wheel profiles, the rails displacement because of widening or constriction of rail gauge, rail depressional elasticity, elastic bending of the wheel pair, wheel deformation (the web of the wheel, mainly), as well as rail canting.

When, owing to wobbling or yawing of the track vehicle the transverse displacement of the wheel pair relatively the gauge takes place for the value Δ one must change the expressions for displaced wheel profiles (dotted lines in Fig. 1.) using the formulas:

$$y_j = F_{2b}(x_j) = F_{1b}(x_j - \Delta), \quad (3)$$

$$y_j = F_{2n}(x_j) = F_{1n}(x_j + \Delta). \quad (4)$$

To define the initial contact point of the wheel and the rail it becomes necessary to find the minimal distance between the correspondent profiles of wheel and rail, as shown in Fig. 1. For example, for the inner wheel-rail pair for $i=1, \dots, m$ it becomes necessary to minimize

$$h_b(x_i) = \frac{x_i - x_j}{x_{j+1} - x_j} [F_{2b}(x_{j+1}) - F_{2b}(x_j)] + F_{2b}(x_j) - f_b(x_i). \quad (5)$$

where $x_{j-1} \leq x \leq x_{j+1}$, when index j can be measured beginning from 1 up to k (the interpolation node quantity for the wheel profile). The desired location of the wheel pair relatively to the gauge can be found this way. Tread profiles (dash-dot line in Fig. 1.) are expressed by mathematic dependencies

$$y_j = F_b(x_j) = F_{z_b}(x_j) - h_b^{\min} \quad (6)$$

$$y_j = F_n(x_j) = F_{z_n}(x_j) - h_n^{\min} \quad (7)$$

Touch-point coordinates that correspond h_b^{\min} and h_n^{\min} define r_b and r_n (wheel local radii in the initial contact points for inner and outer wheels correspondently). Thus, absolute value of relative longitudinal slippage of wheel along the inner rail is

$$\eta_b = \frac{r_n}{r_b} \left(1 - \frac{s_1}{R} \right) - 1 \quad (8)$$

or along the outer rail is

$$\eta_n = \frac{r_b}{r_n} \left(1 + \frac{s_1}{R} \right) - 1 \quad (9)$$

This absolute value to a great extent determines the rate value of wheel and rail surface wear. The location of initial contact points corresponds the disposition of heavily worn areas.

Another significant factor which influences the wear rate of rail and wheel working surfaces are the values of contact stresses on the contact areas of working surfaces. Discovered points of initial contact allow to simplify substantially the search for contact stresses for actual surfaces. To elucidate this condition one must apply to the new calculation diagram (Fig. 2.) where the wheel-rail couple (the outer one, correspondently to Fig. 1.) is displayed. The computations would be made for the wheel only because the actual rail geometry is defined similarly. Then, from the relation (7) one must turn to the functional dependency

$$y = F_m - f(x), \quad (10)$$

which displays the actual wheel profile in the coordinate plane xoy (Fig. 2.). This sort of dependency with r_m is the wheel flange maximum radius is taken for convenience of usage. Functional dependency (10) assumes that a definite interpolating manner is specified for curvature presentation according to the formula (7). Splines may be used, for example. Then, radius vector being drawn to the arbitrariness point on the wheel surface would be discovered as follows:

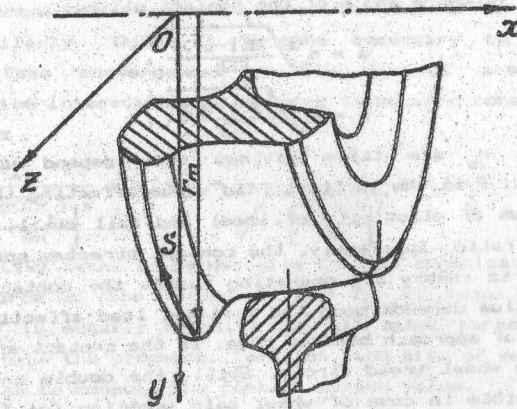


Fig. 2.

$$\vec{r} = \begin{pmatrix} x \\ y \\ z \end{pmatrix} = \begin{pmatrix} x \\ (r_m - f(x)) \cos \frac{s}{r_m} \\ (r_m - f(x)) \sin \frac{s}{r_m} \end{pmatrix}, \quad (11)$$

where s is the arc length of the current point. This point is counted off along the maximum radius circle beginning from the plane xoy , as it is shown in Fig. 2. Thus, the expression (11) turns to be the parametric representation of a wheel tread. Then, according to the statements of differential geometry one must solve the following characteristic equation in order to calculate the curvatures k :

$$k^2(CBGF^2) + k(2MF - BN - LG) + LN - M^2 = 0, \quad (12)$$

where functions B, F, G, M, L, N are defined as scalar and mixed products of vectors $\vec{r}_x, \vec{r}_s, \vec{r}_{xx}, \vec{r}_{xs}, \vec{r}_{ss}$. As an example

$$\vec{r}_{xx} = \begin{pmatrix} 1 \\ -\frac{df}{dx} \cos \frac{s}{r_m} \\ -\frac{df}{dx} \sin \frac{s}{r_m} \end{pmatrix}, \quad (13)$$

$$B = \vec{r}_x \vec{r}_{xx} = 1 + \left(\frac{df}{dx} \right)^2 \quad (14)$$

Other functions are calculated similarly. Thus, the main wheel and rail curvatures in the initial contact point and their sum Σk being computed one can find (using the Hertz theory) the

semi-axis values a and b of the contact ellipse

$$a = n_a \sqrt{\frac{3(1-\nu^2)P}{E\sum k}} \quad (15)$$

$$b = n_b \sqrt{\frac{3(1-\nu^2)P}{E\sum k}} \quad (16)$$

where n_a , n_b are table ratios that depend upon the main curvatures, P is the vertical load value affecting the wheel, E is the modulus of elasticity of wheel and rail metal, and ν is his Poisson's ratio. Apparently, the contact stresses spread according to the Hertz theory are operating inside the contact area. Their maximum value depends upon the vertical load affecting the wheel. This kind of approach becomes true, if the contact area is located within the wheel tread circle. Still, the double area contact is quite possible in case of wheel pair wobbling for the wheel-rail coupling.

Let us assume that one can compute two local minima $h_b(x_n)$ and $h_b(x_l)$ which would correspond the possible double-area case realization. This assumption may occur in the course of distance discrete series analysis $h_b(x_l)$ according to the formular (5). Apparently, for the actual wheel and rail profiles these points would be disposed in the following manner. One point would be placed in the flange curve area and another one would be disposed on the tread area. Assume, that the vertical force $P_n < P$ is operating within the first area, therefore, the vertical force $P_l = P - P_n$ would manifest itself in the second area. It must be noted that for formulas (15), (16) and further according to the Hertz theory it is necessary to substitute for the summary force of the normal pressure equal to

$$Q_n = P_n \sqrt{1 + \left[\frac{df(x_n)}{dx} \right]^2} \quad (17)$$

parallel with assumption that contact surfaces of the first area are smooth. The force Q_l can be similarly calculated for the second area. Therefore, it becomes possible to find out the normal convergence of the wheel and rail surfaces in the first contact area. The calculation are held using the Hertz theory

$$\delta_n = \frac{1}{2} n_a^3 \sqrt{\frac{9(1-\nu^2)Q_n}{E}} \sum k \quad (18)$$

The table ratio (according to the formular (18) n_a) depends upon

the main curvatures. Said curvatures are defined in the coordinate point x_n . Normal convergence δ_l for the second area may be computed similarly. Thus, it becomes necessary to make the vertical surface convergences in the contact areas (their distances to the interaction point being taken into consideration) equal. That is

$$\frac{\delta_n}{\sqrt{1 + \left[\frac{df(x_n)}{dx} \right]^2}} + h_b(x_n) = \frac{\delta_l}{\sqrt{1 + \left[\frac{df(x_l)}{dx} \right]^2}} + h_b(x_l) \quad (19)$$

The relation (19) turns to be decisive for the organization of the iterative search of the forces P_n and P_l . It means that said relation (19) is equally decisive for all other parameters that allow to evaluate the presence, location, and size of each contact area as well as to compute the contact stress value.

The above mentioned mathematic model of contact interaction of the wheel pair and rail gauge was realised in the software package for the personal computer of the IBM PC AT type. The computer graphics checks the wheel-rail interconnection with any admissible displacement and all wheel contact areas obtained. The dynamic contact interaction for the wheel passing the rail joint was also examined.

A number of new designs for rails and wheels with the reduced degree of contact stresses were developed as a result of these researches. For example, the octoaxle tank cars which rotate within the railway network (Eastern testing ground of the USSR) provided with wheels turned according to the DMetI profile design showed 1.8 fold reduction of the flange wear rate. The usage of wheels with said tread profile being mounted to the industrial type of track vehicle and supplied with the new web form showed the 2.5-3 fold reduction of the flange wear rate. The locomotive wheels are subjected to amplified propulsion mode, still the usage of tyres machined conformly the new design of profiles demonstrate 30-40% reduction of the wear rate. The investigation discovered that the lateral force acting between a wheel flange and a lateral face of a rail during the wheel pair wobbling grew with the higher degree of smoothness. This phenomenon causes the reduction of dynamic contact stresses.